Fine Tuning of Craniofacial Morphology by Distant-Acting Enhancers

Catia Attanasio *et al.*

Science **342**, (2013);
DOI: 10.1126/science.1241006

Fine Tuning of Craniofacial Morphology by Distant-Acting Enhancers

Catia Attanasio, Alex S. Nord, Yiwen Zhu, Matthew J. Blow, Zirong Li, Denise K. Liberton, Harris Morrison, Ingrid Plajzer-Frick, Amy Holt, Roya Hosseini, Sengthavy Phouanenavong, Jennifer A. Akiyama, Malak Shoukry, Veena Afzal, Edward M. Rubin, David R. FitzPatrick, Bing Ren, Benedikt Hallgrímsson, Len A. Pennacchio, Axel Visel*

READ THE FULL ARTICLE ONLINE
http://dx.doi.org/10.1126/science.1241006

Cite this article as C. Attanasio *et al.*, *Science* **342**, 1241006 (2013).
DOI: 10.1126/science.1241006

Introduction: The shape of the face is one of the most distinctive features among humans, and differences in facial morphology have substantial implications in areas such as social interaction, psychology, forensics, and clinical genetics. Craniofacial shape is highly heritable, including the normal spectrum of morphological variation as well as susceptibility to major craniofacial birth defects. In this study, we explored the role of transcriptional enhancers in the development of the craniofacial complex. Our study is based on the rationale that such enhancers, which can be hundreds of kilobases away from their target genes, regulate the spatial patterns, levels, and timing of gene expression in normal development.

Methods: To identify distant-acting enhancers active during craniofacial development, we used chromatin immunoprecipitation on embryonic mouse face tissue followed by sequencing to identify noncoding genome regions bound by the enhancer-associated p300 protein. We used LacZ reporter assays in transgenic mice and optical projection tomography (OPT) to determine three-dimensional expression patterns of a subset of these candidate enhancers. Last, we deleted three of the craniofacial enhancers from the mouse genome to assess their effect on gene expression and craniofacial morphology during development.

Results: We identified more than 4000 candidate enhancer sequences predicted to be active in the developing craniofacial complex. The majority of these sequences are at least partially conserved between humans and mice, and many are located in chromosomal regions associated with normal facial morphology or craniofacial birth defects. Characterization of more than 200 candidate enhancer sequences in transgenic mice revealed a remarkable spatial complexity of in vivo expression patterns. Targeted deletions of three craniofacial enhancers near genes with known roles in craniofacial development resulted in changes of expression of those genes as well as quantitatively subtle but definable alterations of craniofacial shape.

Discussion: Our analysis identifies enhancers that fine tune expression of genes during craniofacial development in mice. These results support that variation in the sequence or copy number of craniofacial enhancers may contribute to the spectrum of facial variation we find in human populations. Because many craniofacial enhancers are located in genome regions associated with craniofacial birth defects, such as clefts of the lip and palate, our results also offer a starting point for exploring the contribution of noncoding sequences to these disorders.

FIGURES IN THE FULL ARTICLE

SUPPLEMENTARY MATERIALS

ADDITIONAL RESOURCES

Genomic data sets, transgenic reporter data, and optical projection tomography data for craniofacial enhancers can be found in the Vista Enhancer Browser (http://enhancer.lbl.gov) and the FaceBase database (http://facebase.org) under the identifiers provided throughout the manuscript.

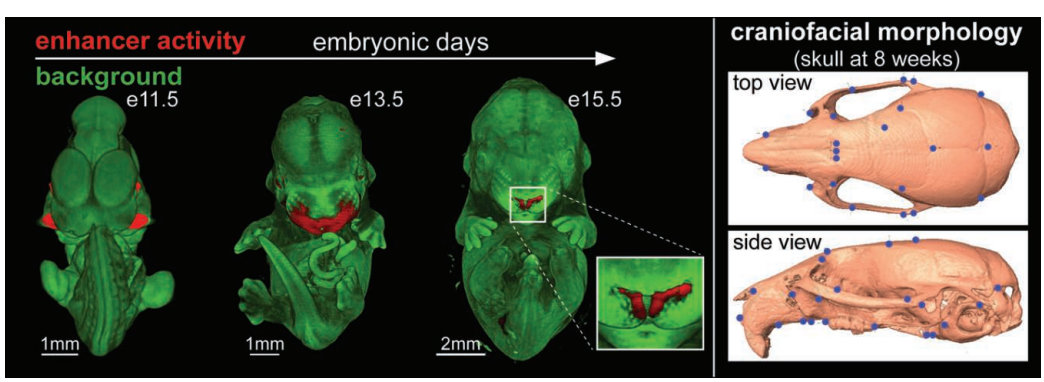

Craniofacial developmental enhancers contribute to craniofacial morphology. We identified distant-acting transcriptional enhancers active in the developing craniofacial complex and studied their activity patterns in detail in transgenic mice (**left**). Selected enhancers were deleted from the genome in mice in order to examine their role in modulating craniofacial morphology, which revealed subtle but significant effects of enhancers on the shape of the face and skull (**right**).

The list of author affiliations is available in the full article online.
*Corresponding author. E-mail: avisel@lbl.gov

Fine Tuning of Craniofacial Morphology by Distant-Acting Enhancers

Catia Attanasio,[1] Alex S. Nord,[1] Yiwen Zhu,[1] Matthew J. Blow,[2] Zirong Li,[3]* Denise K. Liberton,[4] Harris Morrison,[5] Ingrid Plajzer-Frick,[1] Amy Holt,[1] Roya Hosseini,[1] Sengthavy Phouanenavong,[1] Jennifer A. Akiyama,[1] Malak Shoukry,[1] Veena Afzal,[1] Edward M. Rubin,[1,2] David R. FitzPatrick,[5,6] Bing Ren,[3] Benedikt Hallgrímsson,[4,7] Len A. Pennacchio,[1,2] Axel Visel[1,2]†

The shape of the human face and skull is largely genetically determined. However, the genomic basis of craniofacial morphology is incompletely understood and hypothesized to involve protein-coding genes, as well as gene regulatory sequences. We used a combination of epigenomic profiling, in vivo characterization of candidate enhancer sequences in transgenic mice, and targeted deletion experiments to examine the role of distant-acting enhancers in craniofacial development. We identified complex regulatory landscapes consisting of enhancers that drive spatially complex developmental expression patterns. Analysis of mouse lines in which individual craniofacial enhancers had been deleted revealed significant alterations of craniofacial shape, demonstrating the functional importance of enhancers in defining face and skull morphology. These results demonstrate that enhancers are involved in craniofacial development and suggest that enhancer sequence variation contributes to the diversity of human facial morphology.

The shape of the face is one of the features that most distinguishes individual humans from one another. Differences in facial morphology have substantial implications in many areas, including social interaction, psychology, forensics, and clinical genetics (*1*–*3*). The resemblance of facial shapes within families in general, and between monozygotic twins in particular, suggests a major contribution of genetic factors to craniofacial morphology (*4*–*6*). Many protein-coding genes whose disruption causes major aberrations of craniofacial morphology are known. This includes pathological dysmorphologies of the face itself, such as clefts of the lip or palate, as well as distinctive facial features associated with genetic syndromes that are indicative of associated pathologies in other organ systems (*7*–*14*). In contrast to these disease-related genes, only a small number of candidate genes have been implicated in normal variation of craniofacial shape through genome-wide association studies, and collectively they explain only a minute fraction of the morphological variation observed in human populations (*15*–*17*). We are interested to understand how complex traits such as the individualized shape of the face can be modulated in subtle ways while avoiding the often severe consequences associated with protein-coding mutations (*18*).

Recent observations of large numbers of distant-acting transcriptional enhancers in mammalian genomes (*19*–*21*) raise the possibility that these sequences regulate development of structures such as the craniofacial complex. Enhancers can be located hundreds of kilobases away from their target genes and typically have highly restricted in vivo activity patterns. They often control the expression of their target genes in a modular fashion, where different enhancers activate the expression of the same gene in different cell types, anatomical regions, or at different developmental time points. In principle, such complex arrays of enhancers acting on individual genes may provide a general mechanism for the independent fine-tuning of distinct aspects of gene expression in different developmental processes, which in turn may affect specific phenotypic traits, including facial shape (*22*). This model is consistent with the extensive studies of the genes and gene regulatory networks involved in the development of the neural crest, a cell population contributing to multiple tissues, including facial bone and cartilage (*23*). In-depth studies of individual genes involved in neural crest development [e.g., (*24*–*26*)], as well as genome-wide studies of regulatory sequences active in human neural crest cells (*27*), support that many genes involved in craniofacial development are associated with complex regulatory architecture. We used chromatin immunoprecipitation on whole face tissue to explore the genome-wide landscape of craniofacial enhancers in mice, and we studied enhancer involvement in defining mouse craniofacial morphology using transgenic reporter assays and enhancer knockout studies.

Identification of in Vivo Craniofacial Enhancers

To identify craniofacial developmental enhancers on a genome-wide scale, we performed chromatin immunoprecipitation followed by sequencing (ChIP-Seq) analysis on mouse embryonic-day 11.5 (e11.5) facial tissue with the enhancer-associated p300 protein (Fig. 1) (*21*). At this developmental time point, key events of craniofacial development are in progress, including growth and morphogenetic processes affecting the size, shape, and structure of all major craniofacial prominences (*28*, *29*). All major facial subregions were included in this tissue preparation (*30*), building on the previously

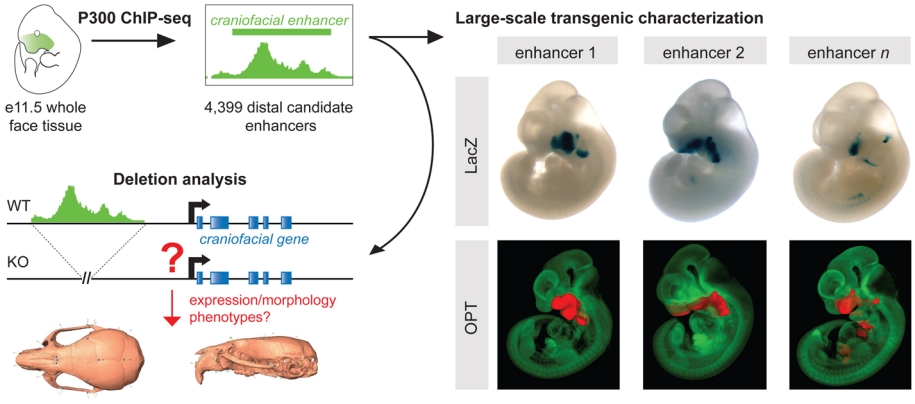

Fig. 1. Study overview. We performed p300 ChIP-Seq on whole mouse face tissue from e11.5 embryos, which identified 4399 putative distant-acting craniofacial enhancers. More than 200 craniofacial candidate enhancers were characterized in depth through LacZ transgenesis in mouse embryos (LacZ; top right), and selected enhancers were further analyzed by means of optical projection tomography (OPT; bottom right). Unstained tissue is shown in green, and LacZ-stained tissue is shown in red. The examples shown here are enhancers mm622, mm924, and mm613. Furthermore, a panel of three enhancers near functionally unrelated genes was studied by means of knockout analysis and detailed skull morphometry in mice. Blue dots indicate standardized morphometric landmarks.

[1]Lawrence Berkeley National Laboratory, Berkeley, CA 94720, USA. [2]U.S. Department of Energy Joint Genome Institute, Walnut Creek, CA 94598, USA. [3]Ludwig Institute for Cancer Research, and Department of Cellular and Molecular Medicine, University of California, San Diego School of Medicine, 9500 Gilman Drive, La Jolla, CA 92093, USA. [4]Department of Cell Biology and Anatomy, McCaig Bone and Joint Institute, University of Calgary, Calgary T2N 4N1, Canada. [5]MRC Human Genetics Unit, MRC Institute for Genetic and Molecular Medicine, University of Edinburgh, Edinburgh EH4 2XU, UK. [6]Royal Hospital for Sick Children, Edinburgh EH9 1LF, UK. [7]Alberta Children's Hospital Research Institute, University of Calgary, Calgary T2N 4N1, Canada.

*Present address: EMD Millipore, 28820 Single Oak Drive, Temecula, CA 92590, USA.
†Corresponding author. E-mail: avisel@lbl.gov

described efficiency of this inclusive approach to identify enhancers with both broad and tightly confined patterns in subregions of developing embryonic structures (*31*, *32*).

Enrichment analysis identified 4399 distal candidate enhancers genome-wide, defined as regions that showed significant p300 binding in craniofacial tissue and were at least 2.5 kb from known transcription start sites (Fig. 2 and tables S1 and S2). Candidate enhancers were located up to 1.4 Mb (median distance, 44 kb) from the nearest known transcript start site, with 38.4% in introns of genes and 54.7% located in noncoding regions outside of genes (intergenic). The majority of candidate enhancers also showed evidence of evolutionary constraint (87.5%) (table S1) and had unique orthologous sequences in the human genome (96.7%). Unbiased ontology analysis (*33*) revealed that candidate craniofacial enhancers are enriched near genes that are known to cause craniofacial phenotypes when deleted in mouse models or mutated in humans (table 1). Candidate craniofacial enhancers were also enriched at loci implicated in human craniofacial traits and birth defects through genome-wide association studies (fig. S1). These observations are consistent with a role of the identified enhancer candidate sequences in the regulation of genes with known roles in craniofacial development. Taken together, these results suggest that thousands of distant-acting enhancers are involved in orchestrating the genome-wide gene expression landscape during craniofacial development.

Large-Scale Transgenic Analysis of Craniofacial Enhancers

ChIP-Seq performed directly on craniofacial tissues provided a genome-wide catalog of sequences that are likely to be active in vivo enhancers during craniofacial development at e11.5. However, this approach does not provide direct insight into the exact activity patterns of individual candidate enhancer sequences. To examine craniofacial enhancer activity patterns in detail, we used transgenic enhancer reporter assays in mice, coupled to high-resolution three-dimensional (3D) mapping of LacZ reporter activities by means of optical projection tomography (OPT) (Fig. 1) (*30*, *34*, *35*). Because many, but not all, in vivo enhancers can be identified through p300 binding (*36*), we also considered sequence conservation (*34*) and proximity to genes or loci with a known role in craniofacial development as additional criteria in the selection of candidate sequences. In total, we tested 205 candidate sequences in transgenic mice, with the majority (123, or 60%) located within or near regions associated with craniofacial development through experimental, genetic, or genome-wide association studies (properties of all tested candidate sequences are provided in table S3). Each candidate enhancer sequence was coupled to a minimal promoter and used to generate multiple transgenic embryos by means of pronuclear injection (*30*). Only patterns that were independently observed in at least three different embryos were

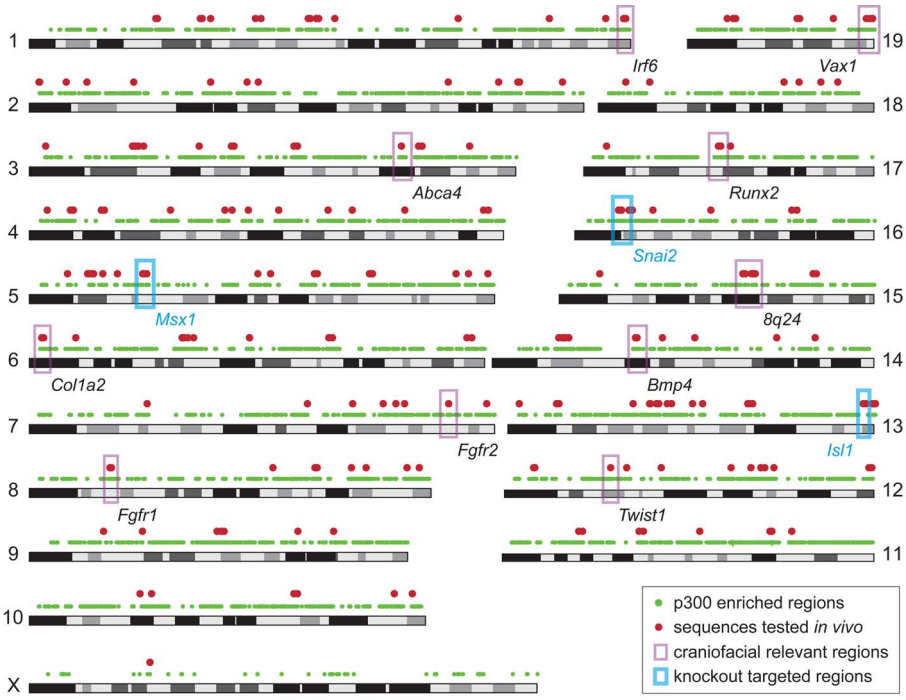

Fig. 2. Genome-wide identification of candidate craniofacial enhancers. Mouse genome graph showing all p300-enriched regions (green dots) and all 281 sequences tested in vivo or reexamined for craniofacial activity in this study (red dots). Examples of selected major craniofacial genes (*55*) and genomic regions [such as regions orthologous to human 8q24 (*43*) and *ABCA4* (*46*)] are highlighted by pink boxes. Known craniofacial loci were generally enriched in candidate sequences and were specifically targeted for sampling in transgenic assays (red dots). The three genomic regions studied by means of knockout analysis are highlighted by blue boxes.

Table 1. Top enriched annotations of mouse and human phenotypes associated with candidate craniofacial enhancers. (**Top**) Ten of the 12 most significantly enriched terms from the mouse phenotype ontology directly relate to craniofacial development. The remaining two phenotypes (abnormal axial skeleton morphology and abnormal skeleton development) relate to general skeleton development, a process that shares key signaling pathways with cranial skeleton development (*58*). (**Bottom**) Six of the 10 most significantly enriched terms from the human phenotype ontology are relevant to craniofacial development. The four remaining phenotypes are all associated with limb abnormalities, which is consistent with previous knowledge of shared developmental pathways during limb and face development (*59*–*61*). In each analysis, only terms exceeding twofold binomial enrichment were considered and ranked by *P* value (binomial raw *P* values).

Rank	Phenotype term	Binomial *P* value	Binomial fold enrichment
	Mouse phenotypes		
1	Abnormal craniofacial morphology	5.8×10^{-110}	2.0
3	Abnormal head morphology	1.78×10^{-88}	2.1
4	Abnormal craniofacial development	3.88×10^{-82}	2.4
5	Abnormal craniofacial bone morphology	1.38×10^{-78}	2.1
6	Abnormal facial morphology	5.58×10^{-78}	2.2
7	Abnormal cranium morphology	3.18×10^{-77}	2.2
9	Abnormal mouth morphology	3.58×10^{-72}	2.3
10	Abnormal orofacial morphology	1.5×10^{-71}	2.3
11	Abnormal viscerocranium morphology	1.0×10^{-62}	2.3
12	Abnormal neurocranium morphology	2.1×10^{-60}	2.5
	Human phenotypes		
2	Malar hypoplasia	3.6×10^{-17}	2.4
3	Abnormality of the midface	7.6×10^{-17}	2.3
5	Abnormal location of ears	5.7×10^{-16}	2.1
7	Low-set ears	1.1×10^{-15}	2.1
8	Abnormality of the fontanelles and cranial sutures	1.2×10^{-15}	2.2
9	Abnormality of the calvarium	1.3×10^{-15}	2.1

considered reproducible. In total, 121 of 205 tested sequences showed reproducible reporter gene expression in at least one craniofacial structure. We further extended the set of in vivo–characterized craniofacial enhancers by reexamining data from previously described large-scale enhancer screens not specifically targeted at craniofacial enhancer discovery (*21*, *31*, *32*, *34*, *37*–*39*), providing an additional 75 craniofacial enhancers (table S3). Transgenic results for the 196 craniofacial enhancers identified or reexamined in this study are available through the Vista Enhancer Browser (http://enhancer.lbl.gov) or the National Institute of Dental and Craniofacial Research (NIDCR) FaceBase consortium web site (http://facebase.org) (*40*).

To gain higher-resolution insight into the 3D activity patterns of craniofacial enhancers in the context of developing embryos, we used optical projection tomography (OPT). In total, representative embryos for 55 craniofacial enhancers, including 48 from this study, were analyzed with OPT. Selected examples of 3D views are provided as supplementary movies (movies S1 to S11). More comprehensive OPT data collections can be interactively explored through a dedicated viewer at the NIDCR FaceBase database (fig. S2) (*40*). Examination of this large set of in vivo–validated and –characterized craniofacial enhancers highlights several salient features and resulting potential applications of these data sets, which we will describe using selected examples. Specifically, this collection of enhancers (i) highlights the diversity of enhancer activity patterns and the regulatory complexity of the genetic code, (ii) enables the dissection of the regulatory landscapes of individual genes known to be involved in craniofacial development, and (iii) provides a starting point for the mechanistic exploration of genomic intervals implicated in craniofacial development through genome-wide association studies.

Diversity of Patterns

To illustrate the reproducibility and diversity of craniofacial activity patterns identified in transgenic embryos, selected examples of enhancers identified in this study are shown in Fig. 3A.

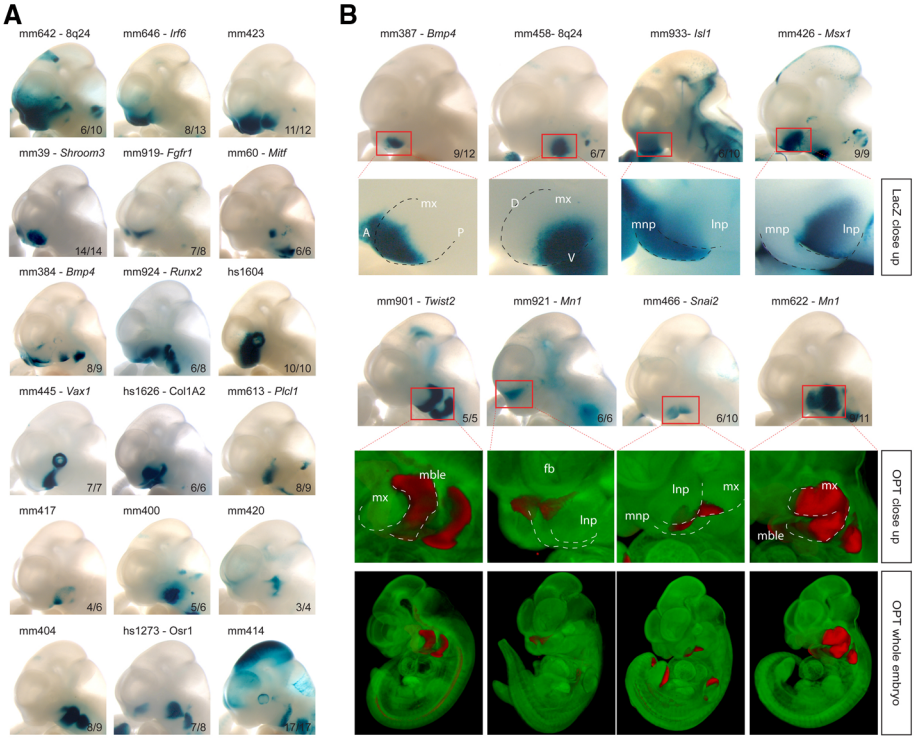

Fig. 3. Transgenic characterization of craniofacial candidate enhancers results in the identification of facial substructure-specific enhancers. (**A**) Selection of 18 reproducible craniofacial enhancers at e11.5 illustrates the broad spectrum of activity patterns observed in vivo. For each tested candidate enhancer, one representative embryo face is shown; the reproducibility of each pattern among multiple transgenic founder embryos is indicated at the right bottom corner of each image. For each element, the nearest relevant craniofacial gene, if any, is also provided. Additional embryo images obtained with each enhancer construct can be viewed at http://enhancer.lbl.gov or http://facebase.org. (**B**) (Top) Four examples of highly restricted specificity to craniofacial substructures. (Bottom) Four examples of internal enhancer activity captured with OPT scanning of LacZ-stained embryos. Green indicates no LacZ activity (enhancer inactive), and red indicates LacZ activity (enhancer active). Embryos have an average crown-rump length of 6 mm. A, anterior; D, dorsal; fb, forebrain; lnp, lateral nasal prominence; mble, mandibular process; mnp, medial nasal prominence; mx, maxillary process; P, posterior; and V, ventral.

For all craniofacial prominences (medial nasal, lateral nasal, maxillary, and mandibular), structure-specific active enhancers were identified (Fig. 3A; a schematic view of the e11.5 mouse face is provided in fig. S4A). In depth analysis of craniofacial activity patterns through the combined use of whole-mount LacZ staining and OPT imaging revealed that in many cases only subregions of these structures were reproducibly targeted by an enhancer. For example, enhancer mm387 drives expression in the anterior part of the maxillary prominence, whereas enhancer mm458 is restricted to a posterior ventral region (Fig. 3B, top). Similar region-specific activities are observed in other facial substructures—such as the nose, where enhancer mm933 is active in the medial nasal prominence, whereas the activity of enhancer mm426 is confined to the lateral nasal prominence (Fig. 3B, top). OPT scans of whole-mount embryos provide additional spatial information about enhancer activity pattern by capturing the activity signal in internal embryonic structures (Fig. 3B, bottom). These data highlight the complexity, diversity, and spatially highly restricted activity patterns of distant-acting enhancer sequences active during craniofacial development.

Regulatory Landscapes of Craniofacial Genes

Systematic screening of individual genomic loci via ChIP-Seq followed by transgenic characterization enables functional dissection of the distant-acting enhancer landscapes of individual genes with known roles in craniofacial development. As an example, mouse *Msx1* and human *MSX1* have been studied for their role in craniofacial development (supplementary text) (*41*). *Msx1* is surrounded by several hundred kilobases of noncoding DNA, which renders the search for distant-acting enhancers challenging. Transgenic testing of seven candidate sequences identified with ChIP-Seq and located up to 235 kb away from the *Msx1* transcription start site resulted in the identification of five distinct craniofacial enhancers potentially regulating its expression (Fig. 4A). At e11.5, each of these enhancers drove patterns that partially recapitulated the endogenous *Msx1* RNA expression. For instance, *Msx1* activity in the second branchial arch and in the maxillary process of the e11.5 embryo is recapitulated by the combined activity of two separate enhancers located at 1 and 235 kb upstream of the promoter (mm426 and hs746) (Fig. 4A). These observations support the notion that complex spatial expression patterns of key developmental genes are driven by modular arrays of distant-acting enhancers (*42*) and highlights the potential of enhancers to provide a mechanism for fine tuning of in vivo gene expression patterns.

Craniofacial Enhancers Within Disease-Associated Intervals

To illustrate the utility of these enhancer data sets in the follow-up of genome-wide association, population-scale sequencing, and candidate locus studies, 50 candidate enhancers mapping to

intervals implicated in craniofacial morphology or orofacial birth defects through human genetic studies were included in the transgenic assays (table S3). Trait-associated variants that map to noncoding genome regions or are not linked to any protein-altering variants are a common challenge in the interpretation of such genetic studies. A prototypical example is a region of human chromosome 8q24 that is devoid of protein-coding genes. A 640-kb stretch located within this region is a major susceptibility locus for cleft palate, with a calculated population attributable risk of 41% (*43*–*45*). Variants at this locus are also significantly linked to normal variation in several facial morphology traits (*16*). We identified four craniofacial enhancer candidate sequences in the mouse genome region orthologous to the human risk interval, two of which drive reproducible craniofacial reporter activity at e11.5 in transgenic mice (Fig. 4B). As a second example, we examined the 1p22 locus. In this interval, markers located near and within the *ABCA4* gene are associated with an increased risk for cleft palate in humans, but it remains unclear whether these variants are linked to deleterious protein-coding mutations of *ABCA4* (*46*, *47*). On the basis of RNA expression data, the neighboring gene *ARHGAP29*, rather than *ABCA4* itself, has been proposed to be causatively involved in craniofacial development (*48*). However, *ARHGAP29* falls outside the genomic boundaries of the risk-associated linkage block. By scanning the region comprising these two genes for possible associated enhancers, we identified a human-mouse conserved sequence in the first intron of *Abca4* that drove highly-reproducible reporter activity in the facial midline, a pattern reminiscent of *Arhgap29* RNA expression, suggesting that this enhancer may drive expression of *Arhgap29* during craniofacial development (Fig. 4C and movie S10) (*49*). A causative effect of sequence or copy number variants in these particular enhancers on craniofacial morphology remains to be demonstrated; furthermore, we cannot exclude the existence of additional enhancer sequences at these loci that were not captured in the present screen. These possible limitations notwithstanding, our results illustrate the utility of collections of validated enhancers as starting points for the mechanistic interpretation of human genetic studies by linking functional genomic and human genetic data sets.

Targeted Deletions of Craniofacial Enhancers

The existence of large numbers of distant-acting enhancers with precise tissue-specific activities during craniofacial development raises the question of their functional impact on craniofacial morphology through the regulation of their respective target genes. To examine such contributions in more detail, we selected three enhancers with highly reproducible craniofacial activity patterns and explored their functions through targeted deletions in mice (Fig. 1). The three enhancers—termed hs1431 (near *Snai2*), hs746 (near *Msx1*), and hs586 (near *Isl1*)—were chosen on the basis of their association with known craniofacial genes (supplementary text) (*7*, *50*, *51*), the robustness of their activity patterns, and the absence of additional known enhancers with overlapping activity near the same gene. Furthermore, the in vivo activity patterns driven by these enhancers partially recapitulate the known expression patterns of their presumptive target genes (Fig. 4A and fig. S3). The enhancers were intentionally chosen from different, functionally unrelated loci in order to provide a representative sample of the genome-wide enhancer data set, rather than an in-depth exploration of a single gene or pathway. All selected enhancers are located at a very long distance from their respective target genes (350, 235, and 190 kb, respectively) and are active in the craniofacial complex through multiple stages of embryonic development (Figs. 4A and 5, fig. S3, and movies S1 to S9).

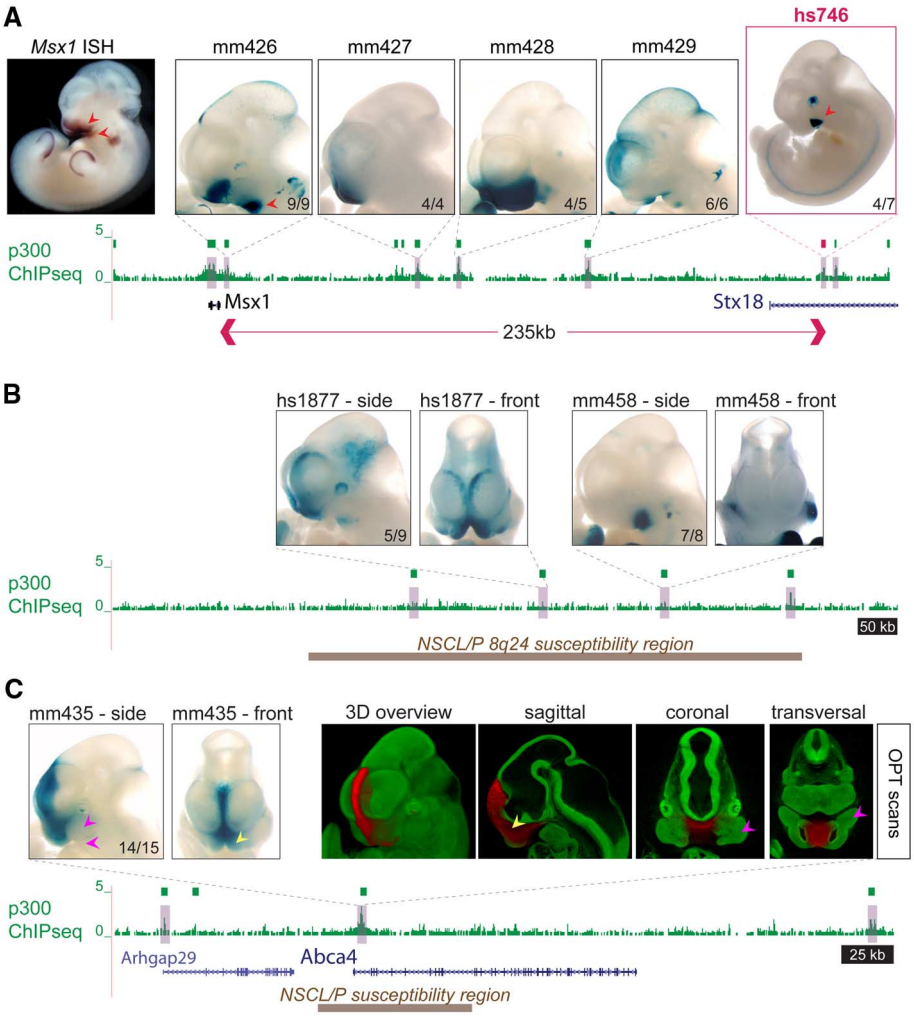

Fig. 4. Regulatory landscapes of craniofacial loci. (**A**) Craniofacial enhancers near *Msx1*, a major craniofacial gene, were identified with p300 ChIP-Seq (green boxes). This included the reidentification of a region proximal to *Msx1* with previously described enhancer activity (mm426) (*56*), as well as four additional, more distal enhancers with complementary activity patterns. For each enhancer, only one representative embryo is shown; numbers indicate reproducibility. Red arrows indicate selected correlations between *Msx1* RNA expression (ISH) and individual enhancers. Red box indicates enhancer hs746, which was further studied by means of knockout analysis. *Msx1* ISH is from Embrys database (http://embrys.jp) (*57*). (**B**) Identification of craniofacial enhancers in the cleft- and morphology-associated gene desert at human chromosome 8q24 (orthologous mouse region shown) (*43*). Brown box indicates the region corresponding to a 640-kb human region associated with orofacial clefts [nonsyndromic cleft lip with or without cleft palate (NSCL/P)] and devoid of protein-coding genes. Two of four candidate enhancers within the region drove craniofacial expression. For each enhancer, lateral and frontal views of one representative embryo are shown. (**C**) Identification of a craniofacial midline enhancer at the cleft-associated susceptibility interval at the ABCA4 locus (*46*). The enhancer is highly active in the nasal prominences (yellow arrows), but not the maxillary or mandible (pink arrows). Embryos have an average crown-rump length of 6 mm.

To test whether these enhancers are important in modulating craniofacial morphology, we created three separate mouse lines carrying deletion alleles for each of the three enhancers using a standard homologous recombination strategy in embryonic stem cells (*30*). Mice homozygous for any of the three enhancer deletions do not display gross craniofacial malformations or other obvious deficiencies. To evaluate the effect of each enhancer deletion on the expression of the presumptive target genes (*Snai2*, *Msx1*, and *Isl1*), we used quantitative reverse transcription polymerase chain reaction to measure transcript levels in different craniofacial structures of individual wild-type and enhancer deletion embryos (littermates) at e11.5 and e13.5 (Fig. 6 and fig. S4). Depending on time-point and substructure, we observed up to 3.9-fold down-regulation ($P = 4 \times 10^{-5}$) of *Snai2* in homozygous Δhs1431 embryos, 1.5-fold down-regulation ($P = 0.015$) of *Msx1* in Δhs746, and 1.3-fold down-regulation ($P = 0.04$) of *Isl1* in Δhs586 (Fig. 6, C and D, and fig. S4E). In all cases, the changes in transcript levels of the respective target gene were confined to subregions in which the enhancer was active. However, not all subregions with enhancer reporter activity showed significant down-regulation of the target gene. These observations raise the possibility of partial functional redundancy between the enhancers studied here and overlapping regulatory activities from gene promoters or additional distant-acting enhancers that were not captured in our genome-wide screen. Regardless of the presence of possible additional regulatory sequences in these genome intervals, these results provide evidence for the requirement of enhancers for normal gene expression during craniofacial development.

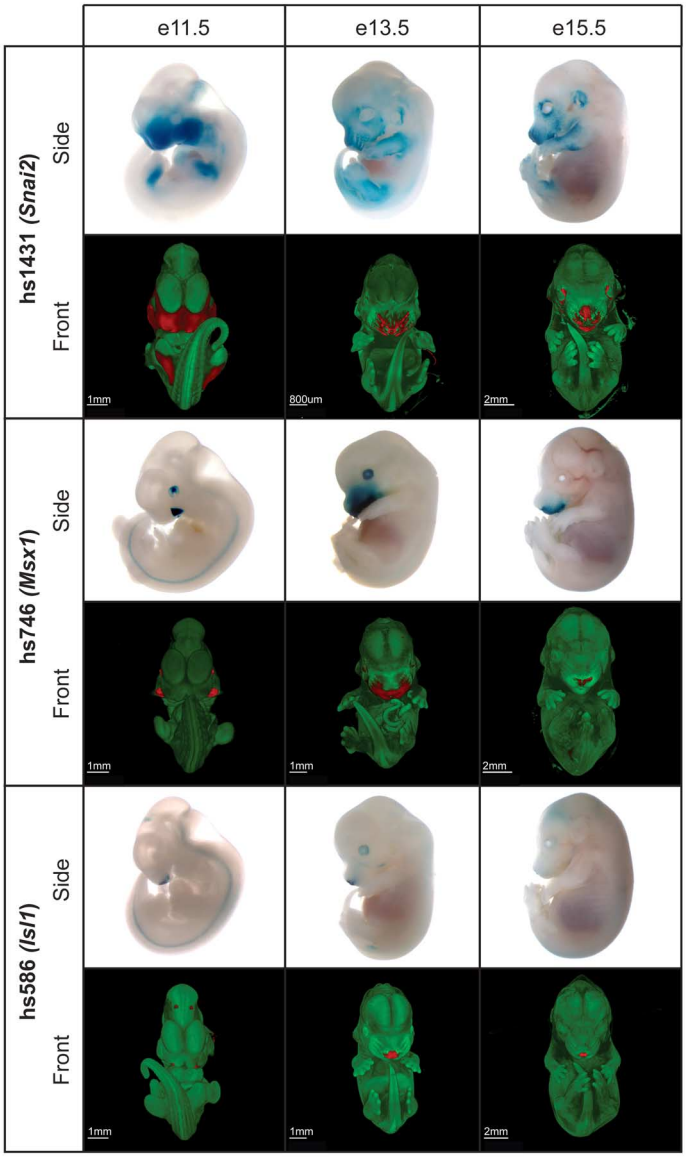

Fig. 5. Developmental activity patterns of three enhancers selected for deletion studies. The in vivo activity of each enhancer was monitored at different stages of development (e11.5, e13.5, and e15.5) (movies S1 to S9). All enhancers were reproducibly active in the craniofacial complex during embryonic development, with spatial changes in activity across stages. Side views are of LacZ-stained whole-mount embryos. Front views are optical projection tomography reconstructed 3D images. Regions of enhancer activity are shown in red.

To examine whether the deletion of these enhancers altered craniofacial morphology, we compared mouse skulls from wild-type and enhancer deletion mice at 8 weeks of age. Because it is challenging to quantify possible differences in craniofacial morphology with visual observation alone, we used micro-computed tomography (micro-CT) to obtain accurate 3D measurements of the skulls. Three cohorts, each consisting of at least 30 mice homozygous for a deletion of one of the three enhancers, were compared with a cohort of 44 wild-type littermates. Micro-CT reconstructions of each mouse head were measured by using 54 standardized skeletal landmarks (fig. S5). The cohorts of wild-type and enhancer deletion mice were compared by using canonical variate analysis (CVA) to identify possible changes in craniofacial morphology resulting from the enhancer deletions (Fig. 7). Procrustes analysis of variance (ANOVA) ($F = 12.0$, $P < 0.0001$) and multivariate ANOVA (Pillau's Trace 2.5, $P < 0.0001$) tests both showed that enhancer deletion genotypes were significantly associated with alterations of craniofacial shape. All individual pair-wise permutation tests (Procrustes distances) between wild-type and enhancer deletion lines revealed significant differences (table S4), with the most pronounced differences observed for Δhs1431 and Δhs746 (both $P < 0.0001$ compared with wild-type). Differences between wild-type, Δhs1431, and Δhs746 mice were also significant after Bonferroni adjustment for the six pairwise comparisons between groups. The largest magnitude of effect on shape was observed for Δhs1431, followed by an intermediate quantitative effect for Δhs746 (Fig. 7B), whereas possible changes in Δhs586 were not statistically significant after correction for multiple hypothesis testing. These results mirror the magnitude of expression phenotypes, which were most pronounced in Δhs1431, followed by intermediate changes in Δhs746 and only a limited expression phenotype observed in Δhs586 (Fig. 6 and fig. S4). These results show that deletion of enhancers can affect craniofacial morphology.

Each enhancer deletion causes a distinct set of differences as compared with wild-type morphology. This is evident from the CVA, in which the first three canonical variates (CV1 to CV3) most clearly separate wild-type mice from Δhs1431, Δhs746, and Δhs586, respectively (Fig. 7). Each enhancer deletion produces phenotypic effects that are not confined to a single feature but involve multiple regions of the skull (Fig. 7C and movies S12 to S20). For example, deletion of hs1431 results in an increase in facial length, a relative increase in the width of the anterior

neurocranium, and a shortening of the anterior cranial base. In contrast, Δhs746 results in a shortening of the face, a widening of the posterior neurocranium, a narrowing of the palate, and shortening of the cranial base. Although both Δhs1431 and Δhs746 have significant effects on facial morphology in structures derived from regions with enhancer activity at e11.5 and e13.5 (Fig. 6), there are also changes in other parts of the skull. These correlated patterns of change are consistent with numerous studies demonstrating that cranium development is a highly integrated process and that variation of the skull is structured by complex interactions between the growing chondrocranium, neurocranium, and other nearby tissues (*52*, *53*). Regardless of the precise molecular pathways and developmental mechanisms that underlie the morphological changes observed upon deletion of these enhancers, these results demonstrate that distant-acting enhancers contribute to the development of craniofacial shape in mammals. The observation of significant but nonpathological alterations of craniofacial morphology as a result of enhancer deletions supports the notion that enhancers contribute to normal variation in facial shape.

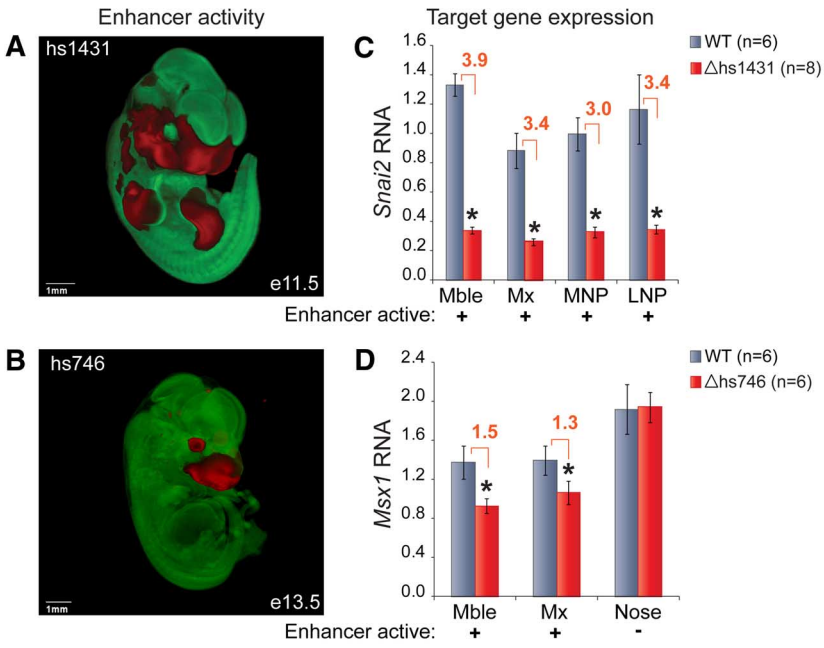

Fig. 6. Expression phenotypes resulting from craniofacial enhancer deletions. (**A** and **B**) In vivo activity pattern of hs1431 (at e11.5) and hs746 (at e13.5). OPT data are represented in red (LacZ, enhancer active) and green (no LacZ, enhancer inactive). (**C** and **D**) Expression levels of enhancer target genes in craniofacial tissues dissected from wild-type (gray) and knockout (red) littermate embryos. Error bars show the variation among individuals of the same genotype (SEM). *$P < 0.05$ (Student t test, one-tailed); Mble, mandibular; Mx, maxillary; MNP, medial nasal process; and LNP, lateral nasal process.

Conclusions

The general shape of the human face and skull, the differences in facial shape between individuals, and the high heritability of facial shape are subjects of broad interest because they have far-reaching implications well beyond basic scientific and biomedical considerations. In this study, we examined the possible impact of distant-acting regulatory sequences on craniofacial morphology. Throughout the genome, we identified several thousand sequences that are likely to be distant-acting enhancers active in vivo during mammalian craniofacial development. Although this epigenomic analysis was performed in the mouse, the vast majority of these enhancer candidate sequences are conserved between mouse and human. Large-scale characterization of more than 200 candidate sequences in transgenic mice showed the versatility of enhancers in orchestrating gene expression during craniofacial development. These observations are consistent with genome-wide analyses of enhancers active in human neural crest cells, as well as studies of regulatory sequences associated with individual members of the neural crest gene regulatory network (*23*–*27*). We also demonstrated that deletion of craniofacial enhancers results in nonpathological but measurable changes in craniofacial morphology in mice. Taken together, these data support that enhancers are involved in determining craniofacial shape. Systematic genome-wide studies of normal morphological variation in human populations are beginning to emerge (*15*–*17*) and will offer the opportunity to compare in vivo–derived genome-wide maps of craniofacial enhancers identified in this study with variation data in order to gain further mechanistic insight into the molecular underpinnings of human facial shape and variation therein.

Beyond the spectrum of normal morphological variation in craniofacial shape, these results also provide a functional genomic framework for the analysis of craniofacial birth defects. We showed that deletion of craniofacial enhancers results in noticeable but nonpathological changes in morphology. Even for Δhs1431, the enhancer deletion resulting in the most severe reduction in craniofacial gene expression, the morphological phenotype was overall much less severe than the pathological changes observed upon deletion of the *Snai2* gene itself (*54*). This milder phenotype is not surprising, considering that remaining baseline activity of the gene was observed in all craniofacial structures examined (Fig. 6A and fig. S4C). Although some enhancer deletions may lead to more severe phenotypes (*26*), these observations highlight the potential of enhancers to modulate craniofacial morphology in quantitatively subtle ways, without the pathological consequences potentially associated with deleterious protein-coding mutations. These results raise the possibility that sequence or copy number variation affecting more than one enhancer of the same gene may cumulatively result in more severe and potentially pathological phenotypes. Isolated examples of sequence variants in distant-acting enhancers associated with malformations such as clefts of the lip or palate have been described (*49*), and there is circumstantial evidence that noncoding sequences, including enhancers, contribute substantially to these processes (*43*). There is partial overlap between loci involved in normal facial shape variation and in craniofacial birth defects, supporting the possibility that some dysmorphologies represent the extreme ends of the normal spectrum of variation (*15*, *16*). The improved genome-wide functional annotation of craniofacial in vivo enhancers obtained through this study is expected to aid not only in the functional exploration of isolated studies of craniofacial dysmorphologies but may also facilitate an understanding of the links between normal and pathological variation in craniofacial shape.

References and Notes

1. K. Christensen, K. Juel, A. M. Herskind, J. C. Murray, Long term follow up study of survival associated with cleft lip and palate at birth. *BMJ* **328**, 1405 (2004). doi: 10.1136/bmj.38106.559120.7C; pmid: 15145797
2. G. L. Wehby, C. H. Cassell, The impact of orofacial clefts on quality of life and healthcare use and costs. *Oral Dis.* **16**, 3–10 (2010). doi: 10.1111/j.1601-0825.2009.01588.x; pmid: 19656316
3. M. Kayser, P. M. Schneider, DNA-based prediction of human externally visible characteristics in forensics: Motivations, scientific challenges, and ethical considerations. *Forensic Sci. Int. Genet.* **3**, 154–161 (2009). doi: 10.1016/j.fsigen.2009.01.012; pmid: 19414162
4. L. A. P. Kohn, The role of genetics in craniofacial morphology and growth. *Annu. Rev. Anthropol.* **20**, 261–278 (1991). doi: 10.1146/annurev.an.20.100191.001401
5. C. Manfredi, R. Martina, G. B. Grossi, M. Giuliani, Heritability of 39 orthodontic cephalometric parameters on MZ, DZ twins and MN-paired singletons. *Am. J. Orthod. Dentofacial Orthop.* **111**, 44–51 (1997). doi: 10.1016/S0889-5406(97)70301-9; pmid: 9009923
6. B. Johannsdottir, F. Thorarinsson, A. Thordarson, T. E. Magnusson, Heritability of craniofacial characteristics between parents and offspring estimated from lateral cephalograms. *Am. J. Orthod. Dentofacial*

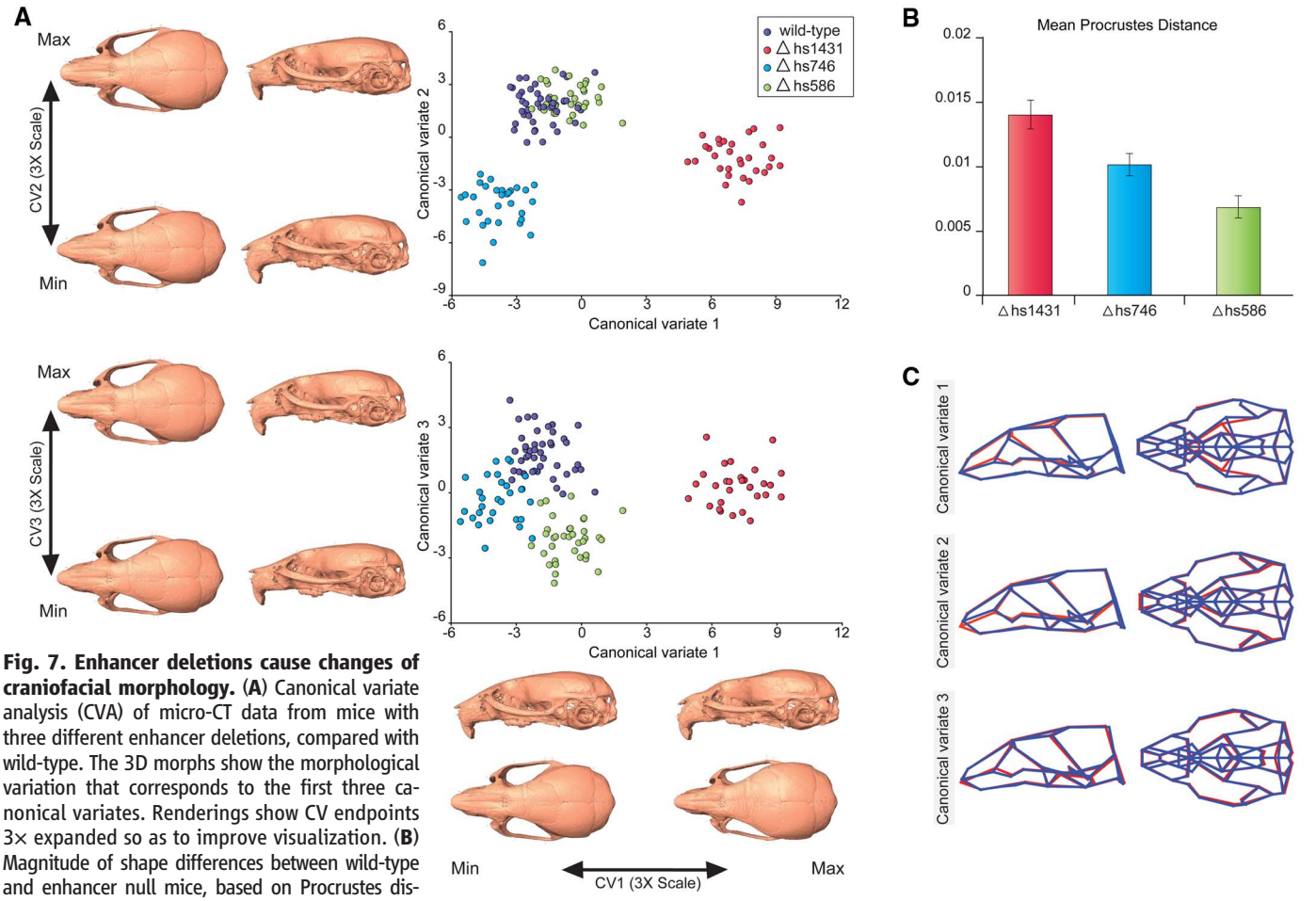

Fig. 7. Enhancer deletions cause changes of craniofacial morphology. (**A**) Canonical variate analysis (CVA) of micro-CT data from mice with three different enhancer deletions, compared with wild-type. The 3D morphs show the morphological variation that corresponds to the first three canonical variates. Renderings show CV endpoints 3× expanded so as to improve visualization. (**B**) Magnitude of shape differences between wild-type and enhancer null mice, based on Procrustes distances (*30*). Error bars indicate SD of shape differences from resampling Procrustes distances across 10,000 iterations. (**C**) Wireframe visualization of the first three canonical variates, which are predominantly driven by morphological differences between wild-type mice and Δhs1431, Δhs746, and Δhs586, respectively. CV endpoints are superimposed as red and blue wireframes, respectively.

Orthop. **127**, 200–207, quiz 260–261 (2005). doi: 10.1016/j.ajodo.2004.07.033; pmid: 15750539
7. I. Satokata, R. Maas, Msx1 deficient mice exhibit cleft palate and abnormalities of craniofacial and tooth development. *Nat. Genet.* **6**, 348–356 (1994). doi: 10.1038/ng0494-348; pmid: 7914451
8. M. J. van den Boogaard, M. Dorland, F. A. Beemer, H. K. van Amstel, MSX1 mutation is associated with orofacial clefting and tooth agenesis in humans. *Nat. Genet.* **24**, 342–343 (2000). doi: 10.1038/74155; pmid: 10742093
9. S. Kondo *et al.*, Mutations in IRF6 cause Van der Woude and popliteal pterygium syndromes. *Nat. Genet.* **32**, 285–289 (2002). doi: 10.1038/ng985; pmid: 12219090
10. S. Suzuki *et al.*, Mutations in BMP4 are associated with subepithelial, microform, and overt cleft lip. *Am. J. Hum. Genet.* **84**, 406–411 (2009). doi: 10.1016/j.ajhg.2009.02.002; pmid: 19249007
11. M. J. Dixon, Treacher Collins syndrome. *Hum. Mol. Genet.* **5**, 1391–1396 (1996). pmid: 8875242
12. S. B. Ng *et al.*, Exome sequencing identifies MLL2 mutations as a cause of Kabuki syndrome. *Nat. Genet.* **42**, 790–793 (2010). doi: 10.1038/ng.646; pmid: 20711175
13. S. B. Ng *et al.*, Exome sequencing identifies the cause of a Mendelian disorder. *Nat. Genet.* **42**, 30–35 (2010). doi: 10.1038/ng.499; pmid: 19915526
14. M. J. Dixon, M. L. Marazita, T. H. Beaty, J. C. Murray, Cleft lip and palate: Understanding genetic and environmental influences. *Nat. Rev. Genet.* **12**, 167–178 (2011). doi: 10.1038/nrg2933; pmid: 21331089
15. S. Boehringer *et al.*, Genetic determination of human facial morphology: Links between cleft-lips and normal variation. *Eur. J. Hum. Genet.* **19**, 1192–1197 (2011). doi: 10.1038/ejhg.2011.110; pmid: 21694738
16. F. Liu *et al.*, A genome-wide association study identifies five loci influencing facial morphology in Europeans. *PLOS Genet.* **8**, e1002932 (2012). doi: 10.1371/journal.pgen.1002932; pmid: 23028347
17. L. Paternoster *et al.*, Genome-wide association study of three-dimensional facial morphology identifies a variant in PAX3 associated with nasion position. *Am. J. Hum. Genet.* **90**, 478–485 (2012). doi: 10.1016/j.ajhg.2011.12.021; pmid: 22341974
18. D. L. Stern, Evolutionary developmental biology and the problem of variation. *Evolution* **54**, 1079–1091 (2000). pmid: 11005278
19. Y. Shen *et al.*, A map of the cis-regulatory sequences in the mouse genome. *Nature* **488**, 116–120 (2012). doi: 10.1038/nature11243; pmid: 22763441
20. J. Zhu *et al.*, Genome-wide chromatin state transitions associated with developmental and environmental cues. *Cell* **152**, 642–654 (2013). doi: 10.1016/j.cell.2012.12.033; pmid: 23333102
21. A. Visel *et al.*, ChIP-seq accurately predicts tissue-specific activity of enhancers. *Nature* **457**, 854–858 (2009). doi: 10.1038/nature07730; pmid: 19212405
22. N. M. Young, H. J. Chong, D. Hu, B. Hallgrímsson, R. S. Marcucio, Quantitative analyses link modulation of sonic hedgehog signaling to continuous variation in facial growth and shape. *Development* **137**, 3405–3409 (2010). doi: 10.1242/dev.052340; pmid: 20826528
23. M. Simões-Costa, M. E. Bronner, Insights into neural crest development and evolution from genomic analysis. *Genome Res.* **23**, 1069–1080 (2013). doi: 10.1101/gr.157586.113; pmid: 23817048
24. S. Bagheri-Fam *et al.*, Long-range upstream and downstream enhancers control distinct subsets of the complex spatiotemporal Sox9 expression pattern. *Dev. Biol.* **291**, 382–397 (2006). doi: 10.1016/j.ydbio.2005.11.013; pmid: 16458883
25. P. Betancur, M. Bronner-Fraser, T. Sauka-Spengler, Genomic code for Sox10 activation reveals a key regulatory enhancer for cranial neural crest. *Proc. Natl. Acad. Sci. U.S.A.* **107**, 3570–3575 (2010). doi: 10.1073/pnas.0906596107; pmid: 20139305
26. H. Yanagisawa, D. E. Clouthier, J. A. Richardson, J. Charité, E. N. Olson, Targeted deletion of a branchial arch-specific enhancer reveals a role of dHAND in craniofacial development. *Development* **130**, 1069–1078 (2003). doi: 10.1242/dev.00337; pmid: 12571099
27. A. Rada-Iglesias *et al.*, Epigenomic annotation of enhancers predicts transcriptional regulators of human neural crest. *Cell Stem Cell* **11**, 633–648 (2012). doi: 10.1016/j.stem.2012.07.006; pmid: 22981823
28. M. H. Kaufman, *The Atlas of Mouse Development* (Academic Press, London, 1992).
29. W. Feng *et al.*, Spatial and temporal analysis of gene expression during growth and fusion of the mouse facial

prominences. *PLOS ONE* **4**, e8066 (2009). doi: 10.1371/journal.pone.0008066; pmid: 20016822
30. Materials and methods are available as supplementary materials on *Science* Online.
31. M. J. Blow *et al.*, ChIP-Seq identification of weakly conserved heart enhancers. *Nat. Genet.* **42**, 806–810 (2010). doi: 10.1038/ng.650; pmid: 20729851
32. A. Visel *et al.*, A high-resolution enhancer atlas of the developing telencephalon. *Cell* **152**, 895–908 (2013). doi: 10.1016/j.cell.2012.12.041; pmid: 23375746
33. C. Y. McLean *et al.*, GREAT improves functional interpretation of cis-regulatory regions. *Nat. Biotechnol.* **28**, 495–501 (2010). doi: 10.1038/nbt.1630; pmid: 20436461
34. L. A. Pennacchio *et al.*, In vivo enhancer analysis of human conserved non-coding sequences. *Nature* **444**, 499–502 (2006). doi: 10.1038/nature05295; pmid: 17086198
35. J. Sharpe *et al.*, Optical projection tomography as a tool for 3D microscopy and gene expression studies. *Science* **296**, 541–545 (2002). doi: 10.1126/science.1068206; pmid: 11964482
36. N. D. Heintzman *et al.*, Histone modifications at human enhancers reflect global cell-type-specific gene expression. *Nature* **459**, 108–112 (2009). doi: 10.1038/nature07829; pmid: 19295514
37. L. Z. Holland *et al.*, The amphioxus genome illuminates vertebrate origins and cephalochordate biology. *Genome Res.* **18**, 1100–1111 (2008). doi: 10.1101/gr.073676.107; pmid: 18562680
38. D. May *et al.*, Large-scale discovery of enhancers from human heart tissue. *Nat. Genet.* **44**, 89–93 (2012). doi: 10.1038/ng.1006; pmid: 22138689
39. A. Visel *et al.*, Ultraconservation identifies a small subset of extremely constrained developmental enhancers. *Nat. Genet.* **40**, 158–160 (2008). doi: 10.1038/ng.2007.55; pmid: 18176564
40. H. Hochheiser *et al.*, The FaceBase Consortium: a comprehensive program to facilitate craniofacial research. *Dev. Biol.* **355**, 175–182 (2011). doi: 10.1016/j.ydbio.2011.02.033; pmid: 21458441
41. S. Alappat, Z. Y. Zhang, Y. P. Chen, Msx homeobox gene family and craniofacial development. *Cell Res.* **13**, 429–442 (2003). doi: 10.1038/sj.cr.7290185; pmid: 14728799
42. A. Visel, E. M. Rubin, L. A. Pennacchio, Genomic views of distant-acting enhancers. *Nature* **461**, 199–205 (2009). doi: 10.1038/nature08451; pmid: 19741700
43. S. Birnbaum *et al.*, Key susceptibility locus for nonsyndromic cleft lip with or without cleft palate on chromosome 8q24. *Nat. Genet.* **41**, 473–477 (2009). doi: 10.1038/ng.333; pmid: 19270707
44. E. Mangold *et al.*, Genome-wide linkage scan of nonsyndromic orofacial clefting in 91 families of central European origin. *Am. J. Med. Genet. A.* **149A**, 2680–2694 (2009). doi: 10.1002/ajmg.a.33136; pmid: 19938073
45. T. Nikopensius *et al.*, Replication of novel susceptibility locus for nonsyndromic cleft lip with or without cleft palate on chromosome 8q24 in Estonian and Lithuanian patients. *Am. J. Med. Genet. A.* **149A**, 2551–2553 (2009). doi: 10.1002/ajmg.a.33024; pmid: 19839039
46. T. H. Beaty *et al.*, A genome-wide association study of cleft lip with and without cleft palate identifies risk variants near MAFB and ABCA4. *Nat. Genet.* **42**, 525–529 (2010). doi: 10.1038/ng.580; pmid: 20436469
47. Q. Yuan, S. H. Blanton, J. T. Hecht, Association of ABCA4 and MAFB with non-syndromic cleft lip with or without cleft palate. *Am. J. Med. Genet. A.* **155A**, 1469–1471 (2011). doi: 10.1002/ajmg.a.33940; pmid: 21567910
48. E. J. Leslie *et al.*, Expression and mutation analyses implicate ARHGAP29 as the etiologic gene for the cleft lip with or without cleft palate locus identified by genome-wide association on chromosome 1p22. *Birth Defects Res. A Clin. Mol. Teratol.* **94**, 934–942 (2012). doi: 10.1002/bdra.23076; pmid: 23008150
49. F. Rahimov *et al.*, Disruption of an AP-2alpha binding site in an IRF6 enhancer is associated with cleft lip. *Nat. Genet.* **40**, 1341–1347 (2008). doi: 10.1038/ng.242; pmid: 18836445
50. K. F. Oram, E. A. Carver, T. Gridley, Slug expression during organogenesis in mice. *Anat. Rec. A Discov. Mol. Cell. Evol. Biol.* **271**, 189–191 (2003). doi: 10.1002/ar.a.10027; pmid: 12552634
51. T. A. Mitsiadis, I. Angeli, C. James, U. Lendahl, P. T. Sharpe, Role of Islet1 in the patterning of murine dentition. *Development* **130**, 4451–4460 (2003). doi: 10.1242/dev.00631; pmid: 12900460
52. D. E. Lieberman, B. Hallgrímsson, W. Liu, T. E. Parsons, H. A. Jamniczky, Spatial packing, cranial base angulation, and craniofacial shape variation in the mammalian skull: Testing a new model using mice. *J. Anat.* **212**, 720–735 (2008). doi: 10.1111/j.1469-7580.2008.00900.x; pmid: 18510502
53. B. Hallgrímsson, D. E. Lieberman, W. Liu, A. F. Ford-Hutchinson, F. R. Jirik, Epigenetic interactions and the structure of phenotypic variation in the cranium. *Evol. Dev.* **9**, 76–91 (2007). doi: 10.1111/j.1525-142X.2006.00139.x; pmid: 17227368
54. S. A. Murray, K. F. Oram, T. Gridley, Multiple functions of Snail family genes during palate development in mice. *Development* **134**, 1789–1797 (2007). doi: 10.1242/dev.02837; pmid: 17376812
55. E. Mangold, K. U. Ludwig, M. M. Nöthen, Breakthroughs in the genetics of orofacial clefting. *Trends Mol. Med.* **17**, 725–733 (2011). doi: 10.1016/j.molmed.2011.07.007; pmid: 21885341
56. A. MacKenzie, L. Purdie, D. Davidson, M. Collinson, R. E. Hill, Two enhancer domains control early aspects of the complex expression pattern of Msx1. *Mech. Dev.* **62**, 29–40 (1997). doi: 10.1016/S0925-4773(96)00646-6; pmid: 9106164
57. S. Yokoyama *et al.*, A systems approach reveals that the myogenesis genome network is regulated by the transcriptional repressor RP58. *Dev. Cell* **17**, 836–848 (2009). doi: 10.1016/j.devcel.2009.10.011; pmid: 20059953
58. B. Balczerski *et al.*, Distinct spatiotemporal roles of hedgehog signalling during chick and mouse cranial base and axial skeleton development. *Dev. Biol.* **371**, 203–214 (2012). doi: 10.1016/j.ydbio.2012.08.011; pmid: 23009899
59. A. Vaahtokari, T. Aberg, J. Jernvall, S. Keränen, I. Thesleff, The enamel knot as a signaling center in the developing mouse tooth. *Mech. Dev.* **54**, 39–43 (1996). doi: 10.1016/0925-4773(95)00459-9; pmid: 8808404
60. E. Koyama *et al.*, Polarizing activity, Sonic hedgehog, and tooth development in embryonic and postnatal mouse. *Dev. Dyn.* **206**, 59–72 (1996). doi: 10.1002/(SICI)1097-0177(199605)206:1<59::AID-AJA6>3.0.CO;2-#; pmid: 9019247
61. A. S. Tucker *et al.*, Conserved regulation of mesenchymal gene expression by Fgf-8 in face and limb development. *Development* **126**, 221–228 (1999). pmid: 9847236

Acknowledgments: The authors thank J. Harkes and M. Satyanarayanan for development of the OPT viewer; S. Shen and H. Hochheiser for integration of the OPT viewer and data sets into FaceBase; and J. Murray, M. Marazita, J. Manak, B. Schutte, and all FaceBase members for help in the selection of relevant craniofacial intervals and comments on results. A.V. and L.A.P. were supported by NIDCR FaceBase grant U01DE020060 and by National Human Genome Research Institute grants R01HG003988 and U54HG006997. C.A. was supported by a Swiss National Science Foundation advanced researcher fellowship. A.S.N. was supported by a F32 NIH/National Institute of General Medical Sciences National Research Service Award fellowship GM105202. B.H. was supported by NIH 1R01DE021708, NIH 1R01DE01963, NIH 1U01DE020054, and Natural Sciences and Engineering Research Council of Canada #238992-11 grants. D.R.F. and H.M. were supported by a UK Medical Research Council core program grant. B.R. was supported by the Ludwig Institute for Cancer Research and NIH grants U54HG006997 and R01HG003991. B.H. was supported by NIH 1R01DE01963. Research was conducted at the E. O. Lawrence Berkeley National Laboratory and performed under Department of Energy contract DE-AC02-05CH11231, University of California. ChIP-Seq data are available through GEO (accession no. GSE49413) and FaceBase.org. In vivo reporter data are available through the Vista Enhancer Browser (http://enhancer.lbl.gov) and FaceBase.org. OPT data, including raw images and interactive 3D viewing option, is available through http://facebase.org. All enhancer reporter vectors, as well as archived surplus LacZ-stained embryos for selected enhancers, are available from the authors. Craniofacial enhancer knockout lines are available through the Mutant Mouse Regional Resource Centers (Δhs1431, MMRRC 03895; Δhs746, MMRRC 03888; and Δhs586, MMRRCC 03894).

Supplementary Materials

www.sciencemag.org/content/342/6157/1241006/suppl/DC1
Materials and Methods
Supplementary Text
Figs. S1 to S6
Tables S1 to S6
References (*62*–*91*)
Movies S1 to S20

24 May 2013; accepted 20 August 2013
10.1126/science.1241006